NANO LETTERS

2006
Vol. 6, No. 12
2945−2948

Plasmonic Nanoparticle Heterodimers in a Semiembedded Geometry Fabricated by Stepwise Upright Assembly

Hui Wang[†,§] and Naomi J. Halas[*,†,‡,§]

Department of Chemistry, Department of Electrical and Computer Engineering, and the Laboratory for Nanophotonics, Rice University, 6100 Main Street, Houston, Texas 77005

Received October 5, 2006; Revised Manuscript Received October 19, 2006

ABSTRACT

We report the experimental realization of plasmonic heterodimers, pairs of directly adjacent, interacting metallic nanoparticles. A novel fabrication and positioning approach is utilized for the stepwise assembly of upright nanoparticle pairs, where the first nanoparticle is almost entirely embedded in an elastomeric dielectric medium prior to attachment of the second nanoparticle. The plasmon energies of the embedded nanoparticles are red-shifted, and the strongly anisotropic dielectric environment of the semiembedded nanoparticle pairs effectively transforms the structures into plasmonic heterodimers. The asymmetric hybridization of the plasmon modes of differing energies on the constituent nanoparticles of the heterodimer is clearly observed.

The properties of metallic nanostructures have become a topic of major interest and importance in nanoscience. Metallic nanostructures are an important class of subwavelength optical elements that can support collective electronic oscillations, known as plasmons, which can couple strongly to incident light. Numerous recent experimental and theoretical advances in this area are allowing us to understand, in a more comprehensive manner, how electromagnetic fields can be controlled and manipulated at nanoscale dimensions, an emerging field known as plasmonics.[1−5]

Many interesting and useful plasmonic phenomena arise due to the interaction between plasmons, whether on directly adjacent nanoparticles, on the various interfaces of individual complex nanostructures, or on nanostructures in close proximity to structures such as metallic films or wires. Interacting plasmons give rise to a wide variety of important properties in nanosystems: electromagnetic transport in waveguide geometries;[6] intense electromagnetic focusing in interparticle junctions, or "hot spots", useful for surface enhanced spectroscopies;[7] "tunable" plasmon resonances of metallic nanostructures such as nanoshells, nanoeggs, nanorice, or nanomatryushkas;[8−12] and increased optical coupling efficiencies into macroscopic waveguiding structures due to excitation of virtual state plasmons.[13] A useful and practical concept advancing our understanding of interacting plasmons has been plasmon hybridization: that plasmons mix and hybridize precisely as if they were wave functions of simple atoms and molecules.[14] On the basis of the plasmon hybridization picture, a pair of strongly coupled, closely adjacent nanoparticles can be understood as an artificial diatomic molecule, in many respects the simplest model system for systematic studies of plasmon interactions.[15]

The importance of the nanoparticle dimer geometry was first recognized from a theoretical point of view in the early 1980s,[16] stimulating further theoretical investigations of this geometry ever since.[15,17−20] Experimentally, the controllable fabrication of nanoparticle dimers remains a significant experimental challenge. One of the most extensively used techniques for fabrication of plasmonic dimers is high-resolution electron beam lithography, where the fabrication of tiny yet reproducible interparticle gaps tests the resolution limits of this top-down approach.[17,21,22] Nanoparticle dimers assembled using molecular linkers such as DNA provide additional chemical approaches with the potential for greater control over particle−particle interactions through precise molecular control over interparticle distances.[23] Heterodimers, strongly interacting nanoparticle pairs with differing plasmon resonant energies, have proven significantly more difficult to fabricate than pairs of identical nanoparticles. Although functional DNA linkers have been shown to provide routes to the assembly of asymmetric nanoparticle pairs, this approach has not yielded the close geometries required for strong coupling and hybridization between the individual constituent nanoparticles of the heterodimer complex. Moreover, chemical assembly methods for dimer structures have not yet been used to produce oriented nanoparticle pairs *en*

* Corresponding author. E-mail: halas@rice.edu.
† Department of Chemistry.
‡ Department of Electrical and Computer Engineering.
§ Laboratory for Nanophotonics.

10.1021/nl062346z CCC: $33.50
Published on Web 11/04/2006

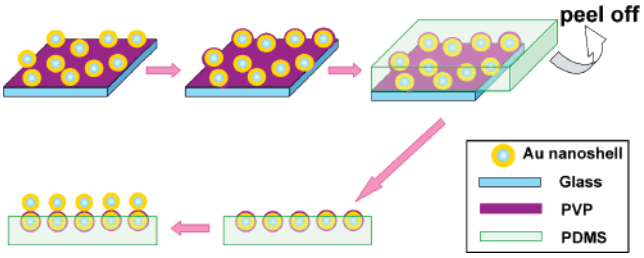

Figure 1. Schematic illustration of the fabrication of nanoshell dimers.

masse, a capability that would facilitate the bottom-up incorporation of more complex nanoparticle assemblies into macroscopic functional materials or nanosystems. For example, such capabilities would greatly facilitate the manufacturability of large-area optical and infrared metamaterials.[24,25]

Here we report the fabrication and characterization of plasmonic heterodimers using a stepwise assembly method for fabricating semiembedded nanoparticle pairs, that is, where one of the two nanoparticles is submerged in an elastomeric dielectric medium. We utilize nanoshells, spherical metallodielectric core−shell nanoparticles with geometrically tunable plasmon resonances, as the nanoparticle "atoms" with which we construct our dimer structures.[8,26] When pairs of identical nanoparticles are assembled in this semiembedded geometry, the presence of the dielectric medium surrounding one of the two nanoparticles preferentially shifts its plasmon resonance so that the resulting structure is strongly asymmetric, hence, a heterodimer. Here we exploit the property that nanoshells have significantly greater surface plasmon resonance shifts upon change in dielectric embedding medium than a corresponding solid spherical metallic nanoparticle.[27−29] Hybridization between the asymmetric plasmon modes of the two constituent individual nanoshells is clearly observed, resulting in bright bonding and antibonding dimer plasmon modes. We also show that this same fabrication approach can be used to assemble heterodimer structures directly, using two different nanoparticles. The use of this semiembedded geometry to create heterodimers through symmetry reduction of homodimer structures, all with the same order and orientation, and over a macroscopic sample size, is a particularly straightforward and systematic way to enable the observation of plasmon hybridization in the heterodimer geometry using extremely straightforward optical techniques.

In Figure 1, the fabrication procedure for semiembedded Au nanoshell dimers is schematically illustrated, and scanning electron micrographs of the fabrication at various stages in the process are illustrated in Figure 2. The silica-core Au-shell nanoparticles were fabricated following a previously reported seed-mediated electroless plating method.[8] The nanoshells were then immobilized onto poly(4-vinylpyridine) (PVP) functionalized glass substrates as a monolayer of isolated nanoshells (see Figure 2A).[29,30] The average interparticle distance is much larger than the diameter of the nanoshells, therefore, the lateral plasmon interactions between the nanoshells, or the assembled nanoshell dimers, are negligible. The surface of these immobilized nanoshells was further functionalized with a PVP layer, which served as the

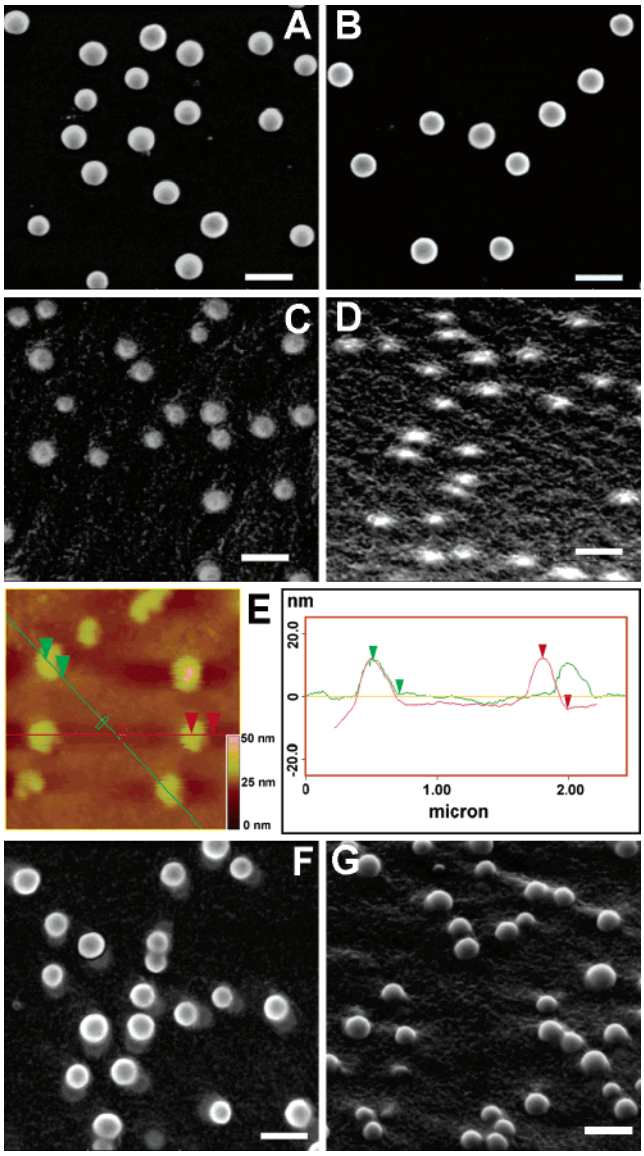

Figure 2. (A) SEM image of monolayer of Au nanoshells (95 ± 10 nm core radius, 17 ± 2 nm shell thickness) immobilized on PVP-glass. (B) SEM image of the monolayer of PVP-functionalized Au nanoshells. (C) Top-view (tilt = 0°) and (D) side-view (tilt = 45°) SEM images and (E) AFM image of Au nanoshells partially imbedded in PDMS. (F) Top-view (tilt = 0°) and (G) side-view (tilt = 45°) SEM images of the nanoshell dimers. The scale bars in the SEM images represent 400 nm.

interparticle linker/spacer between Au nanoshells in the final assembled dimers. Then poly(dimethyl siloxane) (PDMS) elastomer was poured over the immobilized and PVP-functionalized nanoshells and left to stand for nominally 5 h at 353 K for curing. Once cured, the PDMS could be peeled off the substrate, resulting in a PDMS film with partially embedded, PVP-functionalized nanoshells. Such a PDMS embedding and molding technique has also been previously utilized to embed spherical silver nanoparticles.[31,32] The embedded nanoshells exhibit a much darker contrast than the nanoshells exposed in air in the top-view SEM image (Figure 2C), and the partial embedded geometry is clearly observable in the side-view SEM image (Figure 2D). These partially embedded, PVP-functionalized nanoshells protruded nominally 15 nm from the surface of PDMS in this case,

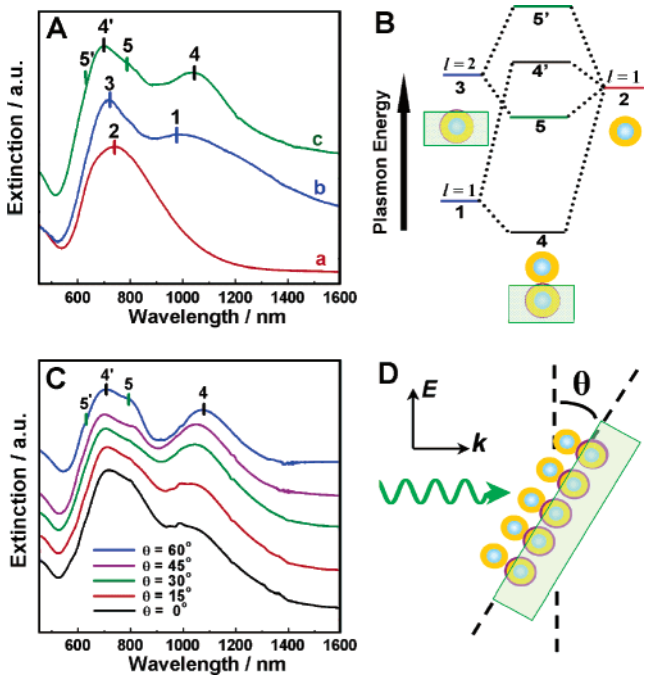

Figure 3. Plasmonic properties of nanoshell dimers. (A) Extinction spectra of nanoshells on glass slide exposed in air (a), the nanoshells partially embedded in PDMS (b), and the nanoshell dimers (c). Measurements were performed using unpolarized incident light at normal incident direction with respect to the surface of the PDMS slab. (B) Energy diagram showing the schematics of how the plasmon modes of two individual nanoshells hybridize to form dimer plasmon modes. (C) Angular-dependent extinction spectra of the nanoshell dimers illuminated by a linearly polarized incident light. (D) The incident direction, polarization direction, and the measurement geometry of the angular-dependent extinction measurements.

according to the AFM image (Figure 2E), indicating that only approximately 7% of the nanoshell surface area is exposed in this sample. Nanoshell dimer structures were subsequently formed upon immersion of the embedded nanoshell film in a solution of Au nanoshells, where PVP provides the attachment in the interparticle junction. Because the embedded, PVP-functionalized nanoshell surfaces barely protrude from the PDMS slab, the binding between the nanoshells in solution and the embedded nanoshells occurs in a 1:1 stoichiometry. The completed structure exhibits a high yield of semiembedded nanoparticle pairs in a well-defined upright orientation, with the dimer axis perpendicular to the PDMS slab surface (Figure 2F,G). The yield of the nanoshell dimers fabricated in this manner is nominally 80% according to the SEM images of our samples. Assuming that the PVP layers formed on Au nanoshell surfaces have the same thickness as those on planar Au surfaces, which can be precisely measured by ellipsometry, the interparticle spacing of the nanoshell dimers is approximately 3.5 nm,[13] a size regime that is small enough for strong plasmon coupling between the two nanoshells in each nanoparticle pair to occur.

Figure 3A shows the extinction spectra of a monolayer of isolated, dispersed nanoshells supported on a glass slide in air (a), the layer of dispersed nanoshells partially embedded in PDMS prior to dimer assembly (b), and the nanoshell dimers (curve c). All of these measurements were performed using unpolarized light at normal incidence with respect to the surface of the PDMS slab. In the present studies, although the two nanoshell constituents of each dimer have the same inner and outer shell radius dimensions $[r_1, r_2] = [95, 112]$ nm, respectively, they possess different plasmon resonance frequencies and multipolar moments because of their different dielectric environments. The spectral peak of the dipole plasmon resonance ($l = 1$) of the nanoshells in air (2) occurs at ~740 nm, while the dipole resonance frequency of the embedded nanoshells (1) is red-shifted to nominally 970 nm, with the additional appearance of a strong quadrupole mode ($l = 2$) at 718 nm due to the significantly increased refractive index of the surrounding medium (PDMS). The plasmon hybridization energy diagram of this heterodimer system is shown in Figure 3B. Here, the individual nanoshell dipolar plasmons (denoted 1 and 2) interact with each other to form hybridized bonding (4) and antibonding (4′) dipolar dimer plasmons that shift to lower and higher energies, respectively, relative to the individual nanoshell dipolar plasmon modes. For a heterodimer system, both the bonding and antibonding dipolar dimer plasmon modes are observable because the dipole and multipolar moments of the individual nanoshells are different.[19] In contrast, in the homodimer systems consisting of two identical nanoshells, only the bonding dimer plasmon is observable due to the zero dipole net moment formed between the two nanoshells for the antibonding mode.[19] The quadrupole mode of the nanoshell embedded in PDMS (denoted as 3) is also observed to hybridize with the dipole mode (2) of the air-side nanoshell, giving rise to additional bright hybridized bonding (5) and antibonding (5′) modes. Modes 5 and 5′ are experimentally observable as two shoulders, one on either side of the 4′ mode at ~790 and ~630 nm respectively, where they contribute to the strongly asymmetric profile of the 4′ plasmon line shape. All of the hybridized dimer plasmon modes can be clearly observed in (c) in Figure 3A.

With polarized incident light, the UV−vis−NIR extinction spectroscopy of this heterodimer film provides additional information regarding the plasmonic interaction of the heterodimer complex due to the orientationally dependent nature of the dimer plasmons. Polarized light provides a powerful tool for investigating the alignment or orientation of optically active anisotropic nanostructures.[31,33] Figure 3C shows the angular-dependent extinction spectra of the nanoshell dimers illuminated by polarized light. The experimental geometry of the angular-dependent extinction spectroscopic measurements are schematically shown in Figure 3D. Maximal coupling between nanoshells occurs when the electric field of the incident pulse is aligned parallel to the dimer axis.[15,19] As the angle θ increases, the bonding dipolar dimer plasmon (4) intensifies and progressively red-shifts, while the antibonding dipolar dimer plasmon blue-shifts slightly, indicating increased plasmon coupling between the two nanoshells. This trend has been predicted previously by the plasmon hybridization model and numerical electrodynamical calculations (FDTD).[15,19] Moreover, the interaction between the dipole plasmon resonance of the nanoshells in air (2) and quadrupole mode of the embedded nanoshells (3) also increases in strength with increasing θ. At $\theta = 45°$ and 60°, the 5 and 5′ modes appear as shoulders on the longer

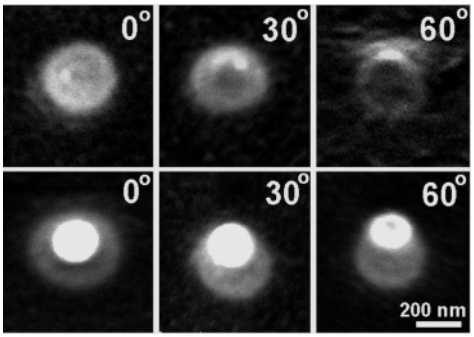

Figure 4. SEM images of (top) a nanoshell partially embedded in PDMS and (bottom) a nanoshell heterodimer consisting of two nanoshells with different core and shell dimensions. The images were taken using tilt = 0°, 30°, and 60°.

and shorter wavelength side of peak 4′, respectively. As we have reported recently, the increased hybridization due to symmetry-breaking in individual plasmonic nanostructures (nanoeggs) also introduces similar broadening and asymmetry in the line shapes of plasmon peaks in their extinction spectra.[11] In addition, for nanoparticles and assemblies with dimensions exceeding the electrostatic limit, phase retardation effects are likely to introduce additional asymmetry and complexity to the spectral line shapes.[34]

It is important to note that this stepwise assembly method can be used to fabricate truly asymmetric nanoparticle pairs in upright and equivalent orientations (Figure 4). This image reveals a nanoshell heterodimer AB where A consists of a $[r_1, r_2] = [140, 160]$ nm nanoshell and B consists of a $[r_1, r_2] = [60, 76]$ nm nanoshell. The angle-dependent images clearly show the two nanoparticles directly adjacent to each other. The plasmon modes of A and B were shifted too far off resonance with respect to each other to show evidence of hybridization in this case.

In summary, we have developed an efficient and versatile stepwise benchtop assembly method for the fabrication of nanoparticle heterodimers and have clearly observed plasmon hybridization in our assembled plasmonic heterodimer system. This method can be widely adapted to fabricate oriented dimers of other geometries of metals and because PVP provides a general binding mechanism for metallic molecules onto a variety of varying material substrates, it is likely to be useful for the assembly of oriented heterodimers of differing materials, with possible semiconductor, polymer, or magnetic nanoparticle constituents. Alternatively, by varying the linker molecules used in the assembly of oriented nanoparticle pairs, one can likely construct oriented molecular rulers to probe interparticle distances in oriented nanoparticle pairs with a new degree of precision.[23] The ease with which this assembly method can be used to produce pairs of nanoparticles all in the same upright orientation and ordering with respect to a substrate is likely to provide a general approach to the assembly of nanoparticles into more complex, bottom-up functional materials and nanosystems.

Acknowledgment. We gratefully acknowledge Professor Peter Nordlander for constructive discussion on the plasmon hybridization theory. This work is supported by Air Force Office of Scientific Research grant F49620-03-C-0068, National Science Foundation (NSF) grant EEC-0304097, the Texas Institute for Bio-Nano Materials and Structures for Aerospace Vehicles funded by NASA Cooperative Agreement no. NCC-1-02038, Robert A. Welch Foundation grant C-1220, and Multidisciplinary University Research Initiative (MURI) grant W911NF-04-01-0203.

Supporting Information Available: Experimental details. This material is available free of charge via the Internet at http://pubs.acs.org.

References

(1) Xia, Y. N.; Halas, N. J. *MRS Bull*. **2005**, *30* (5), 338−344.
(2) Maier, S. A.; Brongersma, M. L.; Kik, P. G.; Meltzer, S.; Requicha, A. A. G.; Atwater, H. A. *Adv. Mater*. **2001**, *13*, 1501−1505.
(3) Barnes, W. L.; Dereux, A.; Ebbesen, T. W. *Nature* **2003**, *424*, 824−830.
(4) Ozbay, E. *Science* **2006**, *311*, 189−193.
(5) Ebbesen, T. W.; Lezec, H. J.; Ghaemi, H. F.; Thio, T.; Wolff, P. A. *Nature* **1998**, *391*, 667−669.
(6) Maier, S. A.; Atwater, H. A. *J. Appl. Phys*. **2005**, *98*, 011101.
(7) Michaels, A. M.; Jiang, J.; Brus, L. *J. Phys. Chem. B* **2000**, *104*, 11965−11971.
(8) Oldenburg, S. J.; Averitt, R. D.; Westcott, S. L.; Halas, N. J. *Chem. Phys. Lett*. **1998**, *288*, 243−247.
(9) Prodan, E.; Nordlander, P. *Nano Lett*. **2003**, *3*, 543−547.
(10) Radloff, C.; Halas, N. J. *Nano Lett*. **2004**, *4*, 1323−1327.
(11) Wang, H.; Wu, Y.; Lassiter, B.; Nehl, C.; Hafner, J. H.; Nordlander, P.; Halas, N. J. *Proc. Natl. Acad. Sci. U.S.A*. **2006**, *103*, 10856−10860.
(12) Wang, H.; Brandl, D. W.; Le, F.; Nordlander, P.; Halas, N. J. *Nano Lett*. **2006**, *6*, 827−832.
(13) Le, F.; Lwin, N. Z.; Steele, J. M.; Kall, M.; Halas, N. J.; Nordlander, P. *Nano Lett*. **2005**, *5*, 2009−2013.
(14) Prodan, E.; Radloff, C.; Halas, N. J.; Nordlander, P. *Science* **2003**, *302*, 419−422.
(15) Nordlander, P.; Oubre, C.; Prodan, E.; Li, K.; Stockman, M. I. *Nano Lett*. **2004**, *4*, 899−903.
(16) Aravind, P. K.; Nitzan, A.; Metiu, H. *Surf. Sci*. **1981**, *110*, 189−204.
(17) Su, K. H.; Wei, Q. H.; Zhang, X.; Mock, J. J.; Smith, D. R.; Schultz, S. *Nano Lett*. **2003**, *3*, 1087−1090.
(18) Hao, E.; Schatz, G. C. *J. Chem. Phys*. **2004**, *120*, 357−366.
(19) Oubre, C.; Nordlander, P. *J. Phys. Chem. B* **2005**, *109*, 10042−10051.
(20) Brandl, D. W.; Oubre, C.; Nordlander, P. *J. Chem. Phys*. **2005**, *123*, 024701.
(21) Atay, T.; Song, J. H.; Nurmikko, A. V. *Nano Lett*. **2004**, *4*, 1627−1631.
(22) Gunnarsson, L.; Rindzevicius, T.; Prikulis, J.; Kasemo, B.; Kall, M.; Zou, S. L.; Schatz, G. C. *J. Phys. Chem. B* **2005**, *109*, 1079−1087.
(23) Sonnichsen, C.; Reinhard, B. M.; Liphardt, J.; Alivisatos, A. P. *Nat. Biotechnol*. **2005**, *23*, 741−745.
(24) Shalaev, V. M.; Cai, W. S.; Chettiar, U. K.; Yuan, H. K.; Sarychev, A. K.; Drachev, V. P.; Kildishev, A. V. *Opt. Lett*. **2005**, *30*, 3356−3358.
(25) Shevchenko, E. V.; Talapin, D. V.; Kotov, N. A.; O'Brien, S.; Murray, C. B. *Nature* **2006**, *439*, 55−59.
(26) Prodan, E.; Nordlander, P. *J. Chem. Phys*. **2004**, *120*, 5444−5454.
(27) Prodan, E.; Nordlander, P.; Halas, N. J. *Chem. Phys. Lett*. **2003**, *368*, 94−101.
(28) Sun, Y. G.; Xia, Y. N. *Anal. Chem*. **2002**, *74*, 5297−5305.
(29) Tam, F.; Moran, C. E.; Halas, N. J. *J. Phys. Chem. B* **2004**, *108*, 17290−17294.
(30) Malynych, S.; Luzinov, I.; Chumanov, G. *J. Phys. Chem. B* **2002**, *106*, 1280−1285.
(31) Malynych, S.; Chumanov, G. *J. Am. Chem. Soc*. **2003**, *125*, 2896−2898.
(32) Malynych, S.; Robuck, H.; Chumanov, G. *Nano Lett*. **2001**, *1*, 647−649.
(33) van der Zande, B. M. I.; Koper, G. J. M.; Lekkerkerker, H. N. W. *J. Phys. Chem. B* **1999**, *103*, 5754−5760.
(34) Westcott, S. L.; Jackson, J. B.; Radloff, C.; Halas, N. J. *Phys. Rev. B* **2002**, *66*, 155431.

NL062346Z

Plasmonic nanoparticle heterodimers in a semiembedded geometry fabricated by stepwise upright assembly

Hui Wang and Naomi J. Halas*

Department of Chemistry, Department of Electrical and Computer Engineering, and the Laboratory for Nanophotonics, Rice University, Houston, TX 77005

*Corresponding author. Email: halas@rice.edu

Experimental details:

Tetraethyl orthosilicate (TEOS, 99.9999%), (3-aminopropyl)trimethoxysilane (APTMS, >97%), tetrachloroauric acid ($HAuCl_4 \cdot 3H_2O$), tetrakis hydroxymethyl phosphonium chloride (THPC, 80% solution in water), and poly(4-vinylpyridine) (160 000 MW) were purchased from Sigma-Aldrich (St. Louis, MO). Ammonium hydroxide and ethanol were obtained from Fisher Scientific (Hampton, NH). Silicone elastomer (PDMS, Sylgard 184) was purchased from Dow Corning Corporation. Ultrapure water (18.2 MΩ resistivity) was obtained from a Milli-Q water purification system (Millipore, Billerica, MA). Glass microscope slides were obtained from Gold Seal Products (Portsmouth, NH). All the chemicals were used as received without further purification. Extinction spectra were obtained using a Cary 5000 UV/Vis/NIR spectrophotometer. Scanning electron microscopy (SEM) measurements were performed using a JEOL 6500 scanning electron microscope. Atomic force microscopy (AFM) was performed with a Digital Instruments Nanoscope IIIa in tapping mode using a 3045JVW piezo tube scanner.

The fabrication of Au nanoshells has previously been described in detail.[1] Briefly, colloidal silica nanospheres prepared by the Stöber method [2] were used as the core material. The size of the silica cores was characterized by SEM and dynamic light scattering (DLS) measurements. The surface of the silica particles was then functionalized with APTMS, to generate an amine moiety-coated silica surface, and decorated with tetrakis hydroxymethyl phosphonium chloride stabilized Au nanoparticles [3] (~ 2 nm in diameter). The attached Au colloids act as nucleation sites that catalyze the reduction of $AuCl_4^-$ ions by formaldehyde, resulting in the formation of continuous Au nanoshells. The as-prepared nanoshells were washed through multiple steps of centrifugation and redispersion in Milli-Q water.

The as-fabricated nanoshells were immobilized onto poly(vinylpyridine)-functionalized glass substrates as a monolayer film of isolated nanoshells.[4] Briefly, glass slides were treated in piranha solution (sulfuric acid : hydrogen peroxide, 7:3) and then immersed in a 1% wt. solution of PVP in ethanol for 24 hours. The slides were rinsed thoroughly with ethanol and dried with N_2 gas flow. Then the PVP-functionalized slides were immersed in an aqueous solution of nanoshells for 1 hour. Upon removal from the nanoshell solution, the films were rinsed with ethanol and dried with N_2. This resulted in a monolayer of isolated nanoshells immobilized on the PVP functionalized glass surface. The surface of the immobilized nanoshells can be further functionalized with PVP by immersing the nanoshell films in 1% wt. solution of PVP in ethanol for 12 hours. Then the films were removed from the PVP solution, rinsed thoroughly with ethanol and dried with N_2.

We used PDMS as the polymer mold to fabricate the partially embedded nanoshells. The PDMS was mixed with the curing agent (10:1 v/v) and outgassed under low pressure (100 milliTorr) at ambient temperature for half an hour before use. Then the PDMS was partially cured in an oven at 50 ˚C for 10 min to increase its viscosity. The partially cured PDMS was then poured over the monolaryer of PVP-functionalized nanoshells and further cured at 80 ˚C for 5 hours. Once cured, the PDMS can be peeled off the glass substrates, resulting in a PDMS slab with partially embedded PVP-functionalized nanoshells.

Nanoshell dimers can be fabricated upon the immersion of the embedded nanoshells in Au nanoshell solutions. Typically, we immersed a PDMS slab with partially embedded PVP-functionalized nanoshells in an aqueous solution of nanoshells (~10^9 particle mL^{-1}) for 2h. Then the PDMS slab was removed from the nanoshell solution, rinsed with ethanol and water in sequence, and finally dried with N_2. During this process, each nanoshell in solution can only be anchored exclusively to exposed surface on the top of individual embedded nanoshells. As a result, the as-fabricated nanoshell dimers have well-defined “standing-up” orientation with the dimer axis perpendicular to the PDMS slab surface.

References

(1) Oldenburg, S. J.; Averitt, R. D.; Westcott, S. L.; Halas, N. J. *Chem. Phys. Lett.* **1998**, *288*, 243.
(2) Stober, W.; Fink, A.; Bohn, E. *J. Colloid Interface Sci.* **1968**, *26*, 62.
(3) Duff, D. G.; Baiker, A.; Edwards, P. P. *Langmuir* **1993**, *9*, 2301.
(4) Tam, F.; Moran, C. E.; Halas, N. J. *J. Phys. Chem. B.* **2004**, *108*, 17290.